Equilibrium tropical cyclone size in an idealized state of axisymmetric radiative-convective equilibrium

Daniel R. Chavas * and Kerry Emanuel

Massachusetts Institute of Technology, Cambridge, Massachusetts

* *Corresponding author address:* Daniel R. Chavas, Massachusetts Institute of Technology, 77 Massachusetts Ave. 54-1715, Cambridge, MA 02139.

E-mail: drchavas@gmail.com

ABSTRACT

Abstract

1. Introduction

Our understanding of the dynamics of tropical cyclones (TCs) has improved considerably over the past three decades. The fundamental air-sea interaction instability that underlies their existence has been identified and placed within the context of a more general theory of tropical cyclones as a Carnot heat engine (Emanuel 1986). Furthermore, both theory and relatively simple dynamical models (Emanuel 1995a; Rotunno and Emanuel 1987) can reproduce the characteristic features of mature tropical cyclones, including maximum wind speed, central sea level pressure, and thermodynamic structure. Most recently, Emanuel and Rotunno (2011) derived a full analytical solution for the radial structure of the axisymmetric balanced tropical cyclone wind field at the top of the boundary layer.

However, this latest solution remains defined relative to a single free parameter: the outer radius, r_0. Indeed, despite wide recognition of the sensitivity of both storm surge (Irish et al. 2008) and wind damage (Iman et al. 2005) to storm size, size remains largely unpredictable, and relatively little observational or modeling work has been performed to try to elucidate the factors underlying its variability. In the absence of land interaction, size is observed in nature to vary only marginally during the lifetime of a given tropical cyclone prior to recurvature into the extra-tropics (Merrill 1984; Frank 1977; Chavas and Emanuel 2010; Cheng-Shang et al. 2010), but significant variation exists from storm to storm, regardless of basin, location, and time of year. Size is found to only weakly correlate with both latitude and intensity (Merrill 1984; Weatherford and Gray 1988; Chavas and Emanuel 2010), as the outer and inner core regions appear to evolve nearly independently. Chavas and Emanuel (2010) found that the global distribution of r_0 is approximately log-normal, though distinct median sizes exist within each ocean basin, suggesting that the size of a given TC is not merely a global random variable but instead is likely modulated either by the structure of the initial disturbance, the environment in which it is embedded, or both.

Recent research has begun to explore the sensitivity of storm size to local thermodynamic variables. Observationally, Quiring et al. (2011) combine the Extended Best Track and

NCEP/NCAR Reanalysis datasets to demonstrate that various local environmental variables have at best a secondary influence on the radius of maximum wind (r_{max}) and the radius of gale force winds in the Atlantic basin, with the exception of a positive correlation between mid-level relative humidity and r_{max}. Idealized modeling studies in Hill and Lackmann (2009) and Xu and Wang (2010) found that TCs tend to be larger when embedded in moister mid-tropospheric environments due to the increase in spiral band activity and subsequent generation of diabatic potential vorticity which acts to expand the wind field laterally. Using a simple three-layer axisymmetric model, Smith et al. (2011) showed an optimum in storm size as a function of ambient planetary rotation attributed to the inhibitive effect of inertial stability on boundary-layer inflow as the rotation rate is increased. Finally, the seminal work of Rotunno and Emanuel (1987) found in an idealized axisymmetric framework a strong relationship between the horizontal length scales of the initial and mature vortex.

A dynamical systems approach may provide a path forward in improving our understanding of tropical cyclone size. Tang and Emanuel (2010) demonstrated analytically that tropical cyclone intensity may be viewed as a non-linear dynamical system that evolves towards a stable equilibrium whose value depends on the local environmental and initial conditions. This behavior has been verified in a modeling context on both short time-scales (e.g. Rotunno and Emanuel (1987)) and long time-scales over which the storm's maximum wind speed has achieved statistical equilibrium (Hakim 2011). However, no such theory exists for the dynamical evolution of tropical cyclone structure, and the tropical cyclone at statistical structural equilibrium remains unexplored. This is of particular relevance given the large range of variation in size observed in nature (Chavas and Emanuel 2010).

Thus, this work seeks to build upon the small base of literature on tropical cyclone size by systematically exploring the sensitivity of the structure of an axisymmetric tropical cyclone at statistical equilibrium to the set of relevant model, initial, and environmental dimensional variables. Expanding on the work of Hakim (2011), we perform our analysis in the simplest possible model and physical environment: a highly-idealized state of radiative-

convective equilibrium (RCE). The results of the sensitivity analysis are then synthesized via dimensional analysis to quantify how, at equilibrium, each structural variable of interest scales with the set of relevant input parameters. Section 2 details the methodology, including model description and experimental design. Results and comparison with existing theory are presented in section 3, with the potential implications of key findings discussed in section 4. Finally, section 5 provides a brief summary and conclusions.

2. Methodology

a. Model description

This work employs Version 15 of the Bryan Cloud Model (CM1), a non-hydrostatic atmospheric cloud-system resolving model (CSRM; original version described in Bryan and Fritsch (2002)) that has been applied to the study of a variety of convective systems including topographic flow (Miglietta and Rotunno 2010), tropical cyclones (Bryan and Rotunno 2009b), and mid-latitude squall lines (Parker 2008). CM1 was originally written with the goal of incorporating state of the art numerics and physics, in particular for moist processes, while satisfying near-exact conservation of both mass and energy in a reversible saturated environment. The model is set up in three-dimensions but can also be configured with identical parameters for two-dimensional axisymmetric (radius-height) geometry, a convenient property that will be exploited in this work.

CM1 solves the fully compressible set of equations of motion in height coordinates on an f-plane for flow velocities (u, v, w), non-dimensional pressure (π), potential temperature (θ), and the mixing ratios of water in vapor, liquid, and solid states (q_χ) on a fully staggered Arakawa C-type grid in height coordinates. The model has a rigid lid at the top with a 5-km thick damping layer beneath; similarly, there is a wall at the domain's outer horizontal edge with an adjacent damping layer whose thickness is set to approximately $\frac{1}{15}$ of the domain's width. Model horizontal (x-y) and vertical grid spacing are each constant in the domain.

Model microphysics is represented using the Goddard-LFO scheme based on Lin et al. (1983), which is a mixed-phase bulk ice scheme with prognostic equations for water vapor, cloud water, rainwater, pristine ice crystals, snow, and large ice. For full details, see Bryan and Fritsch (2002). Lastly, in lieu of a comprehensive scheme for radiative transfer, an idealized scheme (discussed below) is imposed due to its simplicity.

Turbulence is parameterized using a Smagorinsky-type closure scheme (Smagorinsky 1963), which assumes steady and homogeneous unresolved turbulence, modified such that different eddy viscosities are used for the horizontal and vertical directions to represent the differing nature of turbulence between the radial and vertical directions in a highly anisotropic system such as in the inner core of a tropical cyclone. In the context of tropical cyclones, turbulence fulfills the critical role of counteracting eyewall frontogenesis by the secondary circulation that, in the inviscid limit, would lead to frontal collapse (Emanuel 1997). Meanwhile, in a three-dimensional RCE state, turbulence has minimal effect on the mean state.

b. Idealized model/environmental RCE set-up

We construct a highly-idealized model and environmental configuration in order to reduce the model atmospheric system to the simplest possible state (i.e. minimal number of dimensional variables) that supports a tropical cyclone. Model horizontal and vertical grid spacings are set to $dx = dy = dr = 4\ km$ and $dz = .625\ km$, respectively, and no grid stretching is applied. Surface pressure is set to 1015 hPa. Radiation is represented simply by imposing a constant cooling rate (which is typical of the clear-sky mean tropical troposphere, see Hartmann et al. (2001)), Q_{cool}, to the potential temperature everywhere in the domain where the absolute temperature exceeds a threshold value, T_{tpp}; below this value,

Newtonian relaxation back to this threshold is applied:

$$\frac{\partial \theta}{\partial t} = \begin{cases} -Q_{cool} & T > T_{tpp} \\ \frac{\theta(T_{tpp}) - \theta}{\tau} & T \leq T_{tpp} \end{cases} \tag{1}$$

where θ is potential temperature, T is absolute temperature, τ is the relaxation timescale (set to 40 days). Thus, all water-radiation feedbacks are neglected. The lower-boundary sea surface temperature, T_{sst}, is set constant. Surface fluxes of enthalpy and momentum are calculated using standard bulk aerodynamic formulae

$$F_k = C_k \rho |\mathbf{u}| (k_s^* - k) \tag{2}$$

$$\tau_s = -C_d \rho |\mathbf{u}| \mathbf{u} \tag{3}$$

where F_k is the surface enthalpy flux, ρ is the near-surface air density, $\mathbf{u}$ is the near-surface (i.e. lowest model level) wind velocity, k is the near-surface enthalpy, k_s^* is the saturation enthalpy of the sea surface, τ_s is the surface stress, and the exchange coefficients for momentum, C_d, and enthalpy, C_k, are set constant, despite their acknowledged real-world dependence on wind-speed (Powell et al. 2003). Finally, some background surface enthalpy fluxes are required to balance column radiative cooling in order to achieve RCE in the absence of significant resolved wind perturbations (such as a tropical cyclone). Because axisymmetric geometry precludes the direct imposition of a background flow, we instead simply add a constant gustiness, u_s, to $\mathbf{u}$ for the model calculation of (2). This set-up is conceptually similar to that of Hakim (2011) with the important exceptions that here we employ a non-interactive radiative scheme and we include background surface fluxes throughout the domain.

This configuration provides a simplified framework for the exploration of equilibrium tropical cyclone structure in RCE. Nolan et al. (2007) found that, in the presence of a "realistic" radiation scheme, the f-plane RCE state depends only on T_{sst}, u_s and very weakly on f. For this work, the idealized radiation scheme introduces two additional degrees of freedom, T_{tpp} and Q_{cool}, to which the RCE state is sensitive. Thus, we initialize each axisymmetric simulation with the vertical profiles of temperature and water vapor calculated as the 70-

100 day time- and horizontal-mean vertical profiles of temperature and water vapor from the corresponding three-dimensional simulation on a 196x196x40 km domain with identical T_{sst}, T_{tpp}, Q_{cool}, and u_s; the RCE state is indeed found to be nearly insensitive to f (not shown) and thus it is held constant at its control value to reduce computational load. This domain size is specifically chosen to be large enough to permit a large number of updrafts but small enough to inhibit convective self-aggregation (Bretherton et al. 2005) over a period of at least 100 days, though absent any water-radiative feedbacks convective aggregation is unlikely anyways. This approach ensures that each axisymmetric simulation begins very close to its "natural" model-equilibrated background state (first emphasized in Rotunno and Emanuel (1987)) and thus is absent any significant stores of available potential energy that may exist by imposing an alternate initial state, such as a mean tropical sounding.

The result of the above methodology is a model RCE atmosphere comprised of a troposphere capped by a nearly isothermal stratosphere at temperature T_{tpp}. More generally, this model tropical atmosphere may be thought of as an extension of the classical fluid system in which a fluid is heated from below and cooled from above (albeit throughout the column), but with two key modifications: 1) the energy input into the system is dependent on wind-speed, thereby permitting the wind-induced surface heat exchange (WISHE) feedback that is fundamental to steady state tropical cyclones (Emanuel 1986); and 2) the energy lost from the system is dependent on an externally-defined temperature threshold, T_{tpp}, which conveniently corresponds to the convective outflow temperature central to the maximum potential intensity theory of tropical cyclones.

c. Potential Intensity in RCE

The architecture of this model RCE state enables the equation for the maximum potential intensity to be reformulated in a useful manner. The generalized potential intensity (Emanuel

2010) is given by

$$V_p^2 = \frac{C_k}{C_d}\frac{T_{sst} - T_{tpp}}{T_{tpp}}(k_0^* - k) \tag{4}$$

Combining (4) with the surface enthalpy flux equation in (2) gives

$$V_p^2 = \frac{T_{sst} - T_{tpp}}{T_{tpp}}\frac{F_k}{\rho C_d |\mathbf{u}|} \tag{5}$$

In RCE, column energy balance requires that the surface enthalpy flux into the column be exactly balanced by the column-integrated radiative cooling, which in this idealized set-up is given by

$$F_k = \int_{p_s}^{0} C_p \frac{\partial T}{\partial t} dp = \int_{p_s}^{0} C_p \frac{\partial \theta}{\partial t}\left(\frac{p}{p_0}\right)^{R_d/C_p} dp \approx C_p Q_{cool}\frac{\overline{\Delta p}}{g} \tag{6}$$

where C_p is the specific heat of air, $\overline{\Delta p}$ is the mean pressure depth of the troposphere, and we have ignored any small contribution from Newtonian relaxation in the stratosphere. Plugging (6) into (5) results in

$$V_p^2 = \frac{T_{sst} - T_{tpp}}{T_{tpp}}\frac{C_p Q_{cool}\overline{\Delta p}}{g\rho C_d |\mathbf{u}|} \tag{7}$$

Thus, (7) makes it readily apparent that potential intensity in RCE with constant tropospheric cooling is a function of four externally-defined parameters: T_{sst}, T_{tpp}, u_s, and Q_{cool}, with the tropospheric thickness Δp primarily a function of T_{tpp}. This fact will be leveraged in the set of experiments detailed below.

d. Initial condition

Bister and Emanuel (1997) demonstrated that the fundamental process during tropical cyclogenesis is the near-saturation of the column at the mesoscale in the core of the nascent storm. Thus, we superpose an initial perturbation upon the background RCE state by saturating the air at constant virtual temperature in a region above the boundary layer bounded by $z = [1.5, 9.375]\ km$ and $r = (0, r_{0_q})$ within a quiescent environment. We also test an initial mid-level vortex of the form used in Rotunno and Emanuel (1987), characterized by a radius of vanishing wind r_{0_u} and a peak wind of $V_{m_0} = 12.5\ ms^{-1}$ at $r_{m_0} = r_{0_u}/5$,

centered at $z = 4.375\ km$ with azimuthal wind speeds above and below decaying linearly to zero over a distance of 2.875 km. However, as is shown below, the two approaches have similar results, and thus for the sake of simplicity we elect to initialize all other simulations with the mid-level moisture anomaly.

e. Control simulation parameter values

For the control simulation, model parameters are set to $C_d = C_k = .0015$, radial mixing length $l_h = 1.5\ km$ (Bryan and Rotunno 2009b), vertical mixing length $l_h = .1\ km$, and $H_{domain} = 25\ km$; domain width is discussed below; environmental parameters are set to $T_{sst} = 300\ K$, $T_{tpp} = 200\ K$, $f = 5 * 10^{-5}\ s^{-1}$, $Q_{cool} = 1\ \frac{K}{day}$, $u_s = 3\ ms^{-1}$; initial condition parameters are set to $r_{0_q} = 200\ km$ and $r_{0_u} = 400\ km$. The control background RCE sounding is displayed in Figure 1. The potential intensity, calculated from the initial RCE sounding using the Emanuel sub-routine with zero boundary layer wind speed reduction and including dissipative heating is $V_p = 93\ ms^{-1}$. This compares very well with the prediction made by (7) of 92 ms^{-1} for $\rho = 1.1\ kgm^{-3}$ and a tropospheric pressure depth of 850 hPa.

The domain size for the control run requires special attention. Prior research modeling tropical cyclones typically place the outer wall of the domain at a distance of 1000-1500 km (e.g. Rotunno and Emanuel (1987); Hakim (2011)). However, as shown in Figure 2, which depicts the quasi-steady radial profile of the azimuthal component of the gradient wind at $z = 1\ km$, storm structure at statistical equilibrium is dramatically influenced by the radius of the outer wall up to an upper bound. Beyond this upper bound, however, the equilibrium storm is largely insensitive to the location of the wall. The theoretical basis underlying the existence of this upper bound is discussed below.

Thus, because the outer wall is purely a model artifact, we set the outer wall conservatively at $L_{domain} = 12288\ km$ for all simulations run herein. This has the added benefit of ensuring that the storm itself is not significantly altering the background environment, which may act to modify the potential intensity from its RCE value.

f. Characterizing equilibrium storm structure

Following the theory presented in Emanuel and Rotunno (2011), we characterize the complete structure of the tropical cyclone wind field at the top of the boundary layer ($z \approx 1\ km$) with three variables: the maximum gradient wind speed, V_m, the radius of maximum gradient wind, r_m, and the outer radius, r_0, where the wind vanishes. Importantly, only one of the size variables, r_m and r_0, is a free variable while the other is given by the analytical solution. All simulations are run for 150 days in order to allow sufficient time for the full tropical cyclone structure to reach statistical equilibrium. We then calculate a 2-day running mean of the radial profile of the azimuthal gradient wind at approximately $z = 1\ km$ (i.e. near the top of the boundary layer), from which we create a time-series of each variable. This time averaging is necessary to reduce noise in the calculation of the gradient wind from the full pressure field, the pitfalls of which are discussed in Bryan and Rotunno (2009a). The equilibrium radial wind profile is defined as the time-mean of the 30-day period after day 60 with the minimum time-variance in V_m. A dynamic equilibrium period is preferable to a static one (e.g. the day 100-150 mean) to account for certain simulations that exhibit significant long-period departures in storm structure from an otherwise statistically-steady state. This approach allows one to check that each variable has independently reached statistical equilibrium.

Unfortunately, even in a modeling environment, direct calculation of r_0 is difficult due to the noisy nature of the very outer edge of the model storm. Thus, here we employ the outer wind structure model derived in Emanuel (2004) to extrapolate radially outwards to r_0 from the radius of $V = .1V_p$, hereafter r_{mid}; Chavas and Emanuel (2010) applied this methodology to the radius of 12 ms^{-1}, but in our case we will simulate storms with a wide range of peak wind speeds, such that in some cases r_{12} may not be far from the radius of maximum winds itself. The model assumes that the flow is steady, axisymmetric, and absent deep convection beyond r_{mid}, resulting in a local balance between subsidence warming and radiative cooling. Furthermore, given that both the lapse rate and the rate of clear-sky radiative cooling are

nearly constant in the real tropics, the equilibrium subsidence velocity, w_{cool}, can be taken to be approximately constant for a given background RCE state. In equilibrium, this subsidence rate must match the rate of Ekman suction-induced entrainment of free tropospheric air into the boundary layer in order to prevent the creation of large vertical temperature gradients across the top of the boundary layer. The radial profile of azimuthal velocity is therefore determined as that which provides the required Ekman suction, and is given by

$$\frac{\partial(rV)}{\partial r} = \frac{2r^2 C_d V^2}{w_{cool}(r_0^2 - r^2)} - fr \tag{8}$$

where r is the radius and V is the azimuthal wind speed. The value of w_{cool} is calculated from the assumed balance between subsidence and radiative cooling

$$w_{cool}\frac{\partial\theta}{\partial z} = Q_{cool} \tag{9}$$

where $\frac{\partial\theta}{\partial z}$ is set to its mean value in the layer $z = 1.5-5\ km$ (i.e. directly above the boundary layer) in the RCE initial sounding. For the control run, this gives $w_{cool} = .27\ cms^{-1}$, which agrees well with the value of .23 obtained by calculating the mean (negative) vertical velocity in the region $r = [400, 800]\ km$ and $z = [1.5, 5]\ km$ from the equilibrium state of the control simulation. Finally, we solve for r_0 in (8) using a shooting method.

g. Experimental approach: parametric sensitivities and dimensional analysis

We begin by running a Control simulation whose parameter values are given above and the evolution of which is discussed below. We then perform a wide range of experiments in which we independently and systematically vary all dimensional parameters deemed relevant to the dynamics of the system: l_h, f, r_{0_q}, r_{0_u}, T_{sst}, T_{tpp}, Q_{cool}, and u_s; the latter four are subsumed within V_p as discussed in Section 3(b). For each of l_h, f, r_{0_q}, and r_{0_u}, we run six simulations relative to the control case: three with the parameter successively halved and three successively doubled from the control value. For V_p, we perform a suite of simulations varying its four input external parameters (Eq. (1)) that spans a reasonable range of values of V_p.

The final scaling results then indicate to which dimensional variables the equilibrium storm structure is systematically sensitive. Dimensional analysis is then applied to quantify the scaling relationship between each structural variable of interest and all relevant dimensional variables simultaneously.

3. Results

a. Control run

Figure 3 displays the time evolution of the 2-day running mean of V_m, r_m, and r_0 for the control simulation as well as estimated time-scales to equilibrium for each individual variable. As noted above, equilibrium is defined simply as the 70-100 day mean value, and the time-scale to equilibrium, τ_x^*, where x is the variable of interest, is defined as the starting time of the first 30-day interval, iterating backwards from day 70, whose mean value is within 10% of the equilibrium value. All three variables exhibit similar qualitative evolutions: rapid increase during genesis to a super-equilibrium value followed by a more gradual decay to equilibrium. However, the degree of excess over equilibrium is largest for r_0 ($\sim$ 70%), moderate for r_m ($\sim$ 50%) and relatively small ($\sim$ 20%) for V_m. In the case of V_m, the fractional overshoot is slightly smaller than the value found in Hakim (2011) of approximately 30% for the same radial turbulent mixing length, though Hakim (2011) analyzed the surface wind rather than the gradient wind near the top of the boundary layer. Moreover, the time-scales to equilibrium for storm size are significantly longer for size ($\tau_{rm}^* = 54\ days$ and $\tau_{r0}^* = 58\ days$) than for intensity ($\tau_V^* = 30\ days$). The details of the transient phase of the structural evolution will be explored in a separate work. Ultimately, the control simulation's equilibrium storm structure is characterized by $V_m^* = 73\ ms^{-1}, r_m^* = 53\ km, r_0^* = 1150\ km$.

These results suggest that modeling tropical cyclones over a period sufficient to achieve quasi-equilibrium in intensity (typically 10-20 days), as is commonly done in the literature, may result in a storm that has not reached structural equilibrium or else has done so artifi-

cially due to the domain-limitation imposed by the model's outer wall.

b. Sensitivity to potential intensity

Prior to exploring the sensitivity of storm structure to the full suite of dimensional parameters, we may first seek to exploit our relation for potential intensity in RCE given by Eq. (7) in order to simplify the dimensional space amenable to testing. Given (7), one may hypothesize that the primary role of the dimensional parameters T_{sst}, T_{tpp}, Q_{cool}, and u_s is to modulate the potential intensity. To test this hypothesis, we explore the sensitivity of storm structure to the potential intensity, the range of values of which is determined by independently varying each of the above four parameters over the following ranges (listed in order of increasing potential intensity; middle value corresponds to the original control case): $T_{sst} = 295, 297.5, 300, 302.5, 305\ K$; $T_{tpp} = 250, 225, 200, 175, 150\ K$; $u_s = 5, 4, 3, 2, 1\ ms^{-1}$; $Q_{cool} = .25, .5, 1, 2, 4\ Kday^{-1}$. For simulations with T_{tpp} colder than the control run value, the model domain height is increased to 30 km to ensure that there is no interference between the convective outflow and the damping layer near the model top.

The resulting scaling of the maximum gradient wind speed at the top of the boundary layer with the potential intensity is shown in Figure 4. In this case, in the absence of environmental conditions that might inhibit intensification (e.g. vertical wind shear, upper ocean mixing), one expects that V_m ought to scale linear with V_p and therefore that the scaling with the four input sub-variables should collapse to this single linear scaling, and this is indeed the case. The fit is particularly tight for potential intensities at or below the control value.

Of greater interest, however, is the question of whether such a collapse is observed in the scaling of the size variables with V_p. Figure 5 displays the scalings for r_m and r_0, which indeed also approximately collapse to a single scaling with V_p, particularly for r_0. The largest spread exists in r_m at large values of potential intensity, though the overall quasi-linear trend remains evident. Moreover, the scalings for Q_{cool} are monotonic in both V_m and r_m but

exhibit some non-linearity, with negative curvature in the former and positive curvature in the latter, suggesting a shift in r_m while conserving angular momentum. Meanwhile, the scaling for r_0 diverges for low values of Q_{cool} due to the direct dependence of the calculated radiative subsidence rate, w_{cool}, used to calculate r_0 in (8) on the radiative cooling rate; smaller values for w_{cool} correspond to larger values for r_0, all else equal. To the extent that this sensitivity is exhibited primarily in the outer region of the storm (i.e. beyond r_{12}), this divergence indicates an important limitation on the simple three-variable representation of storm structure employed here, which does not distinguish between variability for $r_m < r < r_{12}$ and $r > r_{12}$. Finally, there is one obvious outlier: the $T_{sst} = 305\ K$ simulation exhibits an equilibrium storm that is larger and more intense than would be expected from the set of simulations with variable T_{sst} and their associated values for V_p. The reason for this outlier is unclear, but the non-linear jump with increasing T_{sst} may indicate a deficiency due to the coarse vertical resolution within the boundary layer.

Overall, though, the above results in combination indicate that the primary contribution of these four environmental variables to the equilibrium dynamics not only of the maximum gradient wind speed but of the entire storm structure is manifest in the potential intensity.

c. Parametric sensitivity experiments

We may now proceed to the full parametric sensitivity experiments, where we test V_p in lieu of T_{sst}, T_{tpp}, u_s, and Q_{cool} based on the results of the previous section. Figure 8 displays the scaling of each structural variable with the set of relevant input parameters. All three variables exhibit systematic sensitivity (indicated by a non-zero slope) to three parameters: the potential intensity, V_p, the Coriolis parameter, f, and the turbulent radial mixing length, l_h. Meanwhile, the equilibrium structure is insensitive to the initial disturbance structure as indicated by the near-zero slope in the scaling with the length scale of the initial perturbation, regardless of whether this perturbation is in the form of a mid-level positive vorticity anomaly or positive moisture anomaly. Moreover, equilibrium storm structure is insensitive to the

vertical mixing length over the range of values tested here, though for sufficiently large (and likely unphysical) values on the order of the depth of the troposphere, storm structure does indeed become sensitive to this parameter (not shown) as strong vertical mixing across sloped angular momentum contours within the eyewall has a strong impact on the structure of a mature storm.

Closer inspection of the systematic sensitivities reveals some interesting details about the individual scalings. First, as would be expected, V_m is most strongly modulated by the potential intensity, with a simple linear relationship of unit slope. V_m is weakly negatively correlated with the radial mixing length, with maximum wind speed doubling only once over the entire scaling range. This latter sensitivity reflects the simple fact that turbulence, parameterized here as a diffusive mixing in regions of large flow shear, will act primarily in the eyewall region of the storm where wind speed and its radial gradient concurrently reach their largest magnitude, and thus turbulence will act to to reduce the peak wind speeds. Finally, V_m shows a weak and more complex dependence on f: for $f \geq 2.5 * 10^{-5}$, V_m and f are negatively correlated, whereas for $f < 2.5 * 10^{-5}$ the dependence weakens. This optimum in intensity as a function of background rotation rate was also observed by Smith et al. (2011), who attribute this optimum to the trade-off between the increasing background reservoir of angular momentum and the increasing inertial stability, with the latter effect becoming dominant as the Coriolis parameter is made sufficiently large. Indeed, the product of V_m (Figure 8, top panel) and r_m (middle panel) equals the angular momentum at the radius of maximum winds, which remains approximately constant as f is decreased below $2.5 * 10^{-5}$. OUTER BOUNDARY ISSUES FOR VERY LARGE STORM?

Both size metrics, r_m and r_0, exhibit sensitivities to the same parameters as V_m, though with different magnitudes and, in the case of the radial turbulence length scale, opposite sign. For r_m, the parametric scalings are of the same order across all three relevant input parameters, indicating that horizontal turbulence strongly modulates the inner-core structure. Meanwhile, r_0 is strongly modulated by both V_p and f and only weakly modulated by

l_h, the latter an indication that diffusive turbulence will have a lesser impact on the outer structure where gradients in wind speed are much weaker.

d. Dimensional analysis: non-dimensional scaling

The above analysis can be synthesized quantitatively via dimensional analysis. The Buckingham-Pi theorem states that the number of independent non-dimensional parameters in a dimensional system is equal to the difference between the number of independent dimensional parameters and the number of fundamental measures. For our purposes, we have three relevant dimensional parameters, V_p, f, and l_h, and two fundamental measures, distance and time, thereby giving only one independent non-dimensional parameter, C. Moreover, the theorem states that any output dimensional quantity, Y, suitably non-dimensionalized, can be expressed as a function of the set of non-dimensional parameters. For our system, the result is

$$\frac{Y}{Y_{nd}} = f(C) \tag{10}$$

The form of this functional relationship can only be determined by experimentation.

Thus, we exploit this analytical technique using the results from Figure 8, noting that, given the dimensional parameters V_p, f, and l_h, there exists only one relevant non-dimensional number in our system at its equilibrium state:

$$C = \frac{V_p}{f l_h} \tag{11}$$

We choose to non-dimensionalize each structural variable by an appropriate (though arbitrary) scale: V_m by V_p, and r_m and r_0 by $\frac{V_p}{f}$. The scaling between each equilibrium non-dimensional variable and C for a large set of experiments varying two or more of V_p, f, or l_h are displayed in Figure 9. Linear relationships on the log-log plot indicate power-law relationships between the non-dimensional structural variable and the quantity C, with the power-law exponent given by the slope of the line: i.e.

$$\frac{Y}{Y_{nd}} = C^{\alpha} \tag{12}$$

For non-dimensional intensity, radius of maximum gradient winds, and outer radius, we obtain $\alpha_{V_m} = .16$, $\alpha_{r_m} = -.47$, and $\alpha_{r_0} = -.08$, respectively. In all cases, the p-value is close to zero, indicating that the slopes are statistically-significantly different from zero.

Finally, we may now solve for the dimensional relationship for each structural variable by combining (11) and (12) and approximating the exponents for simplicity as $\alpha_{V_m} \approx .15$, $\alpha_{r_m} \approx -.5$, and $\alpha_{r_0} \approx -.1$ to give:

$$V_m \sim V_p^{1.15} \left(f l_h\right)^{-.15} \qquad r_m \sim \left(\frac{V_p}{f}\right)^{\frac{1}{2}} (l_h)^{\frac{1}{2}} \qquad r_0 \sim \left(\frac{V_p}{f}\right)^{.9} (l_h)^{.1} \tag{13}$$

Thus, equilibrium storm intensity is found to scale super-linearly with the potential intensity and is slightly reduced by an increase in either the background rotation rate or the radial turbulent mixing length. The equilibrium radius of maximum gradient wind is found to elegantly scale as the geometric mean of the ratio of the potential intensity to the Coriolis parameter and the radial turbulent mixing length. Finally, the equilibrium outer radius is found to follow a simple quasi-linear scaling with the ratio of the potential intensity to the Coriolis parameter that expands slightly with increasing radial turbulent mixing length.

Clearly radial turbulence plays a significant role in determining the inner core structure of the storm. The super-linear scaling for V_m can be understood in the context of changes in r_m relative to the radial turbulent mixing length: all else equal, a more intense storm is also a larger storm. Because parameterized radial turbulence will act to reduce radial gradients in scalars such as temperature (and thus gradient azimuthal wind speed, through gradient thermal wind balance) over a distance proportional to the prescribed mixing length, a storm with a larger r_m will feel a weaker effective turbulence. For example, if one scales V_p and f equally while keeping l_h constant, the result is constant r_m and a pure linear scaling of V_m – the increase in f maintains a constant storm size and thus a constant effective radial turbulence and thereby eliminates the super-linearity in the scaling of V_m with V_p. The same conclusion is obtained if one scales V_p and l_h equally at constant f.

Moreover, the strong dependence of r_m on l_h also appears to have a straightforward

physical basis related to the strength of turbulence in the eye. As noted by REFERENCE, the simplest model of the radial profile of azimuthal wind in the eye assumes that radial turbulence will rapidly homogenize angular velocity such that the eye will tend towards a state of approximate solid-body rotation, characterized by $V(r) = cr$ where $c = \frac{\partial V}{\partial r}$ is constant. If we assume that $\frac{\partial V}{\partial r} \approx \frac{V_m}{r_m}$, using (15) one can show

$$\frac{\partial V}{\partial r} \sim (l_h)^{.35} \left(\frac{V_p}{f} \right)^{.65} \tag{14}$$

For a given set of environmental parameters, V_p and f, $\frac{\partial V}{\partial r}$ in the eye is a function solely of the radial turbulent mixing length, suggesting that this mixing length scale defines the critical magnitude of the radial gradient in azimuthal winds toward which super-critical radial wind profiles will be rapidly restored by parameterized turbulent mixing. Given a peak wind speed V_m, this process therefore approximately determines r_m.

As a caveat, it is important to recognize that these quasi-linear scalings in log-log space are only shown to be valid over the roughly two orders of magnitude over which C is varied. It is possible that more extreme variation in this parameter may exhibit qualitatively different behavior. However, we believe that these scaling results are robust at least over the subspace of physical parameter values relevant to the atmosphere of an Earth-like planet.

ANGULAR MOMENTUM BUDGET/BALANCE IN EYE TO EXPLAIN THIS?

e. Q_{cool} at constant V_p

FILL ME IN!

f. Estimating l_h

Given the sensitivity of the equilibrium structure, particularly r_m, to the turbulent radial mixing length, an accurate estimation of l_h in the inner core of a real tropical cyclone is important but lacks any theoretical or observational foundation. Thus we follow the work of Bryan and Rotunno (2009b) and attempt to estimate its value by tuning it to match

the steady-state model intensity to the theoretical potential intensity ($93\ ms^{-1}$), which here would dictate a value of $l_h \approx 600\ m$ as compared to optimal estimate of $l_h = 1500\ m$ in Bryan and Rotunno (2009b).

$$V_m \sim C_d^{.2}\ V_p^{1.15}\,(f l_h)^{-.15} \qquad r_m \sim \left(\frac{V_p}{f}\right)^{\frac{1}{2}} (l_h)^{\frac{1}{2}} \qquad r_0 \sim \left(\frac{V_p}{f}\right)^{.9} (l_h)^{.1} \quad (15)$$

g. Comparison to existing theory

Though not widely recognized, existing axisymmetric tropical cyclone theory predicts a scaling for the upper bound on the size of a tropical cyclone. The existence of this theoretical upper bound is most easily understood from a Carnot engine perspective, in which the work required to build the anticyclone aloft increases with increasing storm size, and by conservation of energy there remains less energy available to overcome frictional dissipation at the surface, i.e. a weaker storm (Emanuel 1986). However, the predicted scaling for this upper bound is most tractable in Eq. (16) of Emanuel (1995b), which derives an analytical relationship between the non-dimensional maximum gradient wind speed and the outer radius such that

$$V_m^2 \sim 1 - \frac{1}{4}\gamma r_0^2 \quad (16)$$

where V_m is non-dimensionalized by $\sqrt{\chi_s}$, a modified potential intensity for $C_k = C_d$ (Bister and Emanuel 1998), r_0 is non-dimensionalized by $\frac{\sqrt{\chi_s}}{f}$, and γ is a thermodynamic constant that depends only on the background environment. Thus, this non-dimensionalization explicitly predicts that the upper bound on storm size scales approximately as the ratio of the modified potential intensity to the Coriolis parameter. Indeed, our modeling results confirm this prediction, with a minor modification in the scaling due to radial turbulence.

Additionally, we may use our derived scalings to test the theoretical prediction for frictional dissipiation of angular momentum in the boundary layer. For a reasonably intense vortex, Emanuel and Rotunno (2011) (Eq. (38)) find that the ratio of the initial angular

momentum, $M_0 = \frac{1}{2} f r_0^2$, to the final angular momentum at the radius of maximum winds, $M_f \approx V_m r_m$ is a constant that is solely a function of the ratio of the exchange coefficients

$$\frac{M_f}{M_0} = \left(\frac{1}{2} \frac{C_k}{C_d} \right)^{\frac{1}{2 - \frac{C_k}{C_d}}} \tag{17}$$

*** IS THIS RIGHT? I REALLY SHOULD HAVE THE CONSTANTS OF PROPORTIONALITY IN THERE I THINk *** For $C_k = C_d$, this ratio is simply .5. For comparison, we apply (15) to obtain

$$\frac{M_f}{M_0} \sim 2 \left(\frac{V_p}{f l_h} \right)^{-.15} \tag{18}$$

The small exponent indicates the this ratio is reasonably constant. However, for the parameter values used in our control simulation, (18) gives a value of .69. In order to match the theoretical prediction, the radial turbulent mixing length must be reduced substantially to $l_h = 180\ m$. Alternatively, one may follow the approach of (Bryan and Rotunno 2009b) for estimating l_h and simply try to match V_m to V_p, which in this case results in a value of approximately $l_h = 550\ m$. In either case, the estimate for l_h is significantly lower than the estimated optimal value of 1500 m found in (Bryan and Rotunno 2009b). This is surprising given that the storms simulated here are much larger and thus one would anticipate that the optimal value for l_h would scale accordingly.

4. Discussion

Issues:

- Turbulence parameterization is already noted to be important in determining storm structure (George Bryan paper), but this problem is exacerbated when coupled with the vagaries of modeling storm size, rendering prediction of r_m and V_m very difficult in an axisymmetric framework, particularly for comparison with real storms given the large range of observed storm sizes. Thoughts on resolving this: new parameterizations? In

principle, turbulence mixing length ought to scale with the size of the largest unresolved eddy, which should scale with the r_m (test this?)

- Real storms likely always in transient phase (where initial condition may matter), and large range in observed size distribution cannot be explained by equilibrium results.

- Axisymmetry likely reasonable for modeling the equliibrium storm, but for transient phase is 3d necessary? Rendered difficult given the result here that artificially small domain size has profound impact on storm size

- effects of real radiation and other effects neglected here?

5. Conclusions

This works combines highly idealized modeling with dimensional analysis to systematically quantify the scaling between the structure of a model tropical cyclone at statistical equilibrium and relevant model, initial, and environmental dimensional input parameters. We perform this analysis in a model world whose complexity is reduced so as to retain only the essential physics of the tropical atmosphere while simultaneously capturing the three-dimensional structure of a tropical cyclone with reasonable fidelity: radiative-convective equilibrium in axisymmetric geometry on an f-plane with constant tropospheric cooling, constant background surface wind speed (for the calculation of surface fluxes only), constant surface exchange coefficients for momentum and enthalpy, and constant sea surface and tropopause temperatures. Importantly, this model tropical atmosphere could in principle exist for all time in column-wise radiative-convective equilibrium, in which column-integrated radiative cooling is exactly balanced by surface fluxes of enthalpy, in the absence of a tropical cyclone, though this explicitly does not occur under axisymmetric geometry. Finally, following the theoretical work of Emanuel and Rotunno (2011), we characterize the full structural evolution of the storm by the time-series of three dynamical variables calculated near the top of

the boundary layer: the maximum gradient wind speed, the radius of maximum gradient winds, and the outer radius.

We find here that, under these simplified conditions, the storm structure at statistical equilibrium is a function of only three parameters: the potential intensity, the Coriolis parameter, and the radial turbulent mixing length. Specifically,

- the maximum wind speed scales linearly with the potential intensity, but this scaling is made super-linear (sub-linear) if the ratio of the radius of maximum winds to the radial turbulent mixing length is increased (decreased)

- the radius of maximum winds scales as the geometric mean of the ratio of the potential intensity to the Coriolis parameter and the turbulent radial mixing length

- the outer radius scales nearly linearly with the ratio of the potential intensity to the Coriolis parameter that is weakly modified by radial turbulence

For our control simulation, the time-scale to equilibration is approximately twice as long for storm structure ($\sim$ 60 *days*) as for storm intensity ($\sim$ 30 *days*). The transient stage is characterized by an initial excess over equilibrium that is largest for the outer radius, moderate for the radius of maximum gradient winds, and relatively small for the maximum gradient wind. This period is then followed by a more gradual decay towards equilibrium. The transient storm will be analyzed more thoroughly in a subsequent paper.

There are a number of interesting implications of the findings presented here. First, the long time-scales required for the storm to come reasonably close to structural equilibrium suggests that prior work modeling tropical cyclones out to statistical steady state in intensity are likely not at statistical steady state in structure. Second, and perhaps more importantly, the sensitivity of storm size to the location of the outer wall, typically set to a value of approximately 1500 km, indicates that axisymmetric studies artificially limit the size of their model storm. This is further complicated by the nature of the parameterization of turbulence in axisymmetric geometry that includes a free parameter–the turbulent radial

mixing length–that is largely unconstrained but to which the storm structure, particularly in the inner core, is particularly sensitive.

6. Acknowledgements

Thanks to Greg Hakim, Marty Singh, and Tim Cronin for a number of very useful discussions in the course of this work.

REFERENCES

Bister, M. and K. A. Emanuel, 1997: The genesis of hurricane guillermo: Texmex analyses and a modeling study. *Monthly Weather Review*, **125 (10)**, 2662–2682.

Bister, M. and K. A. Emanuel, 1998: Dissipative heating and hurricane intensity. *Meteorology and Atmospheric Physics*, **65 (3-4)**, 233–240.

Bretherton, C. S., P. N. Blossey, and M. Khairoutdinov, 2005: An energy-balance analysis of deep convective self-aggregation above uniform sst. *Journal of the Atmospheric Sciences*, **62 (12)**, 4273–4292.

Bryan, G. H. and J. M. Fritsch, 2002: A benchmark simulation for moist nonhydrostatic numerical models. *Monthly Weather Review*, **130 (12)**, 2917–2928, doi:10.1175/1520-0493(2002)130⟨2917:ABSFMN⟩2.0.CO;2.

Bryan, G. H. and R. Rotunno, 2009a: Evaluation of an analytical model for the maximum intensity of tropical cyclones. *Journal of the Atmospheric Sciences*, **66 (10)**, 3042–3060.

Bryan, G. H. and R. Rotunno, 2009b: The maximum intensity of tropical cyclones in axisymmetric numerical model simulations. *Monthly Weather Review*, **137 (6)**, 1770–1789, doi:10.1175/2008MWR2709.1.

Chavas, D. R. and K. A. Emanuel, 2010: A quikscat climatology of tropical cyclone size. *Geophysical Research Letters*, **37 (18)**, 10–13.

Cheng-Shang, L., K. K. W. Cheung, F. Wei-Ting, and R. L. Elsberry, 2010: Initial maintenance of tropical cyclone size in the western north pacific. *Monthly Weather Review*, **138 (8)**, 3207–3223.

Emanuel, K., 2010: Tropical cyclone activity downscaled from noaa-cires reanalysis, 1908-1958. *Journal of Advances in Modeling Earth Systems*, **2 (1)**, 1–12.

Emanuel, K. and R. Rotunno, 2011: Self-stratification of tropical cyclone outflow. part I: Implications for storm structure. *Journal of the Atmospheric Sciences*, **68 (10)**, 2236–2249, doi:10.1175/JAS-D-10-05024.1.

Emanuel, K. A., 1986: An air-sea interaction theory for tropical cyclones. part i: Steady-state maintenance. *Journal of the Atmospheric Sciences*, **43 (6)**, 585–605, doi:10.1175/1520-0469(1986)043⟨0585:AASITF⟩2.0.CO;2.

Emanuel, K. A., 1995a: The behavior of a simple hurricane model using a convective scheme based on subcloud-layer entropy equilibrium. *Journal of the Atmospheric Sciences*, **52 (22)**, 3960–3968, doi:10.1175/1520-0469(1995)052⟨3960:TBOASH⟩2.0.CO;2.

Emanuel, K. A., 1995b: Sensitivity of tropical cyclones to surface exchange coefficients and a revised steady-state model incorporating eye dynamics. *Journal of the Atmospheric Sciences*, **52 (22)**, 3969–3976.

Emanuel, K. A., 1997: Some aspects of hurricane inner-core dynamics and energetics. *Journal of the Atmospheric Sciences*, **54 (8)**, 1014–1026.

Frank, W. M., 1977: The structure and energetics of the tropical cyclone i. storm structure. *Monthly Weather Review*, **105 (9)**, 1119–1135.

Hakim, G. J., 2011: The mean state of axisymmetric hurricanes in statistical equilibrium. *Journal of the Atmospheric Sciences*, **68 (6)**, 1364–1386.

Hartmann, D. L., J. R. Holton, and Q. Fu, 2001: The heat balance of the tropical tropopause, cirrus, and stratospheric dehydration. *Geophys. Res. Lett.*, **28 (10)**, 1969–1972, doi:10.1029/2000GL012833.

563 Hill, K. A. and G. M. Lackmann, 2009: Influence of environmental humidity on tropical
564 cyclone size. *Monthly Weather Review*, **137 (10)**, 3294–3315, doi:10.1175/2009MWR2679.
565 1.

566 Iman, R. L., M. E. Johnson, and C. C. Watson, 2005: Sensitivity analysis for computer
567 model projections of hurricane losses. *Risk Analysis*, **25 (5)**, 1277–1297.

568 Irish, J. L., D. T. Resio, and J. J. Ratcliff, 2008: The influence of storm size on hurricane
569 surge. *Journal of Physical Oceanography*, **38 (9)**, 2003–2013.

570 Lin, Y.-L., R. D. Farley, and H. D. Orville, 1983: Bulk parameterization of the snow field in
571 a cloud model. *Journal of Climate and Applied Meteorology*, **22 (6)**, 1065–1092.

572 Merrill, R. T., 1984: A comparison of large and small tropical cyclones. *Monthly Weather*
573 *Review*, **112 (7)**, 14081418.

574 Miglietta, M. M. and R. Rotunno, 2010: Numerical simulations of low-cape flows over a
575 mountain ridge. *Society*, **67 (7)**, 2391–2401.

576 Nolan, D. S., E. D. Rappin, and K. A. Emanuel, 2007: Tropical cyclogenesis sensitivity to
577 environmental parameters in radiativeconvective equilibrium. *Society*, **2107 (629)**, 2085–
578 2107.

579 Parker, M. D., 2008: Response of simulated squall lines to low-level cooling. *Journal of the*
580 *Atmospheric Sciences*, **65 (4)**, 1323.

581 Powell, M. D., P. J. Vickery, and T. A. Reinhold, 2003: Reduced drag coefficient for high
582 wind speeds in tropical cyclones. *Nature*, **422 (6929)**, 279–283.

583 Quiring, S., A. Schumacher, C. Labosier, and L. Zhu, 2011: Variations in mean annual
584 tropical cyclone size in the atlantic. *Journal of Geophysical Research*, **116 (D9)**, D09 114.

585 Rotunno, R. and K. A. Emanuel, 1987: An air-sea interaction theory for tropical cyclones.
586 part ii: Evolutionary study using a nonhydrostatic axisymmetric numerical model. *Journal*
587 *of the Atmospheric Sciences*, **44 (3)**, 542–561.

588 Smagorinsky, J., 1963: General circulation experiments with the primitive equa-
589 tions. *Monthly Weather Review*, **91 (3)**, 99–164, doi:10.1175/1520-0493(1963)091⟨0099:
590 GCEWTP⟩2.3.CO;2.

591 Smith, R. K., C. W. Schmidt, and M. T. Montgomery, 2011: An investigation of rotational
592 influences on tropical-cyclone size and intensity. *Quarterly Journal of the Royal Meteoro-*
593 *logical Society*, **137 (660)**, 1841–1855, doi:10.1002/qj.862.

594 Tang, B. and K. Emanuel, 2010: Midlevel ventilation's constraint on tropical cyclone inten-
595 sity. *Journal of the Atmospheric Sciences*, **67 (6)**, 1817–1830, doi:10.1175/2010JAS3318.1.

596 Weatherford, C. and W. Gray, 1988: Typhoon structure as revealed by aircraft reconnais-
597 sance. part i: Data analysis and climatology. *Monthly Weather Review*, **116 (8)**, 1032–
598 1043.

599 Xu, J. and Y. Wang, 2010: Sensitivity of the simulated tropical cyclone inner-core size
600 to the initial vortex size*. *Monthly Weather Review*, **138 (11)**, 4135–4157, doi:10.1175/
601 2010MWR3335.1.

List of Figures

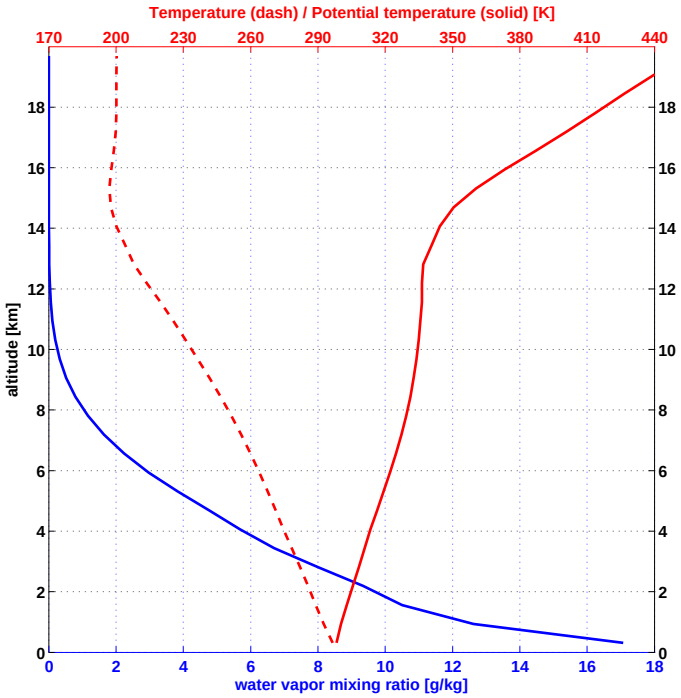

FIG. 1. Radiative-convective equilibrium vertical profile of temperature (red dashed), potential temperature (red solid), and water vapor (blue) for the Control simulation.

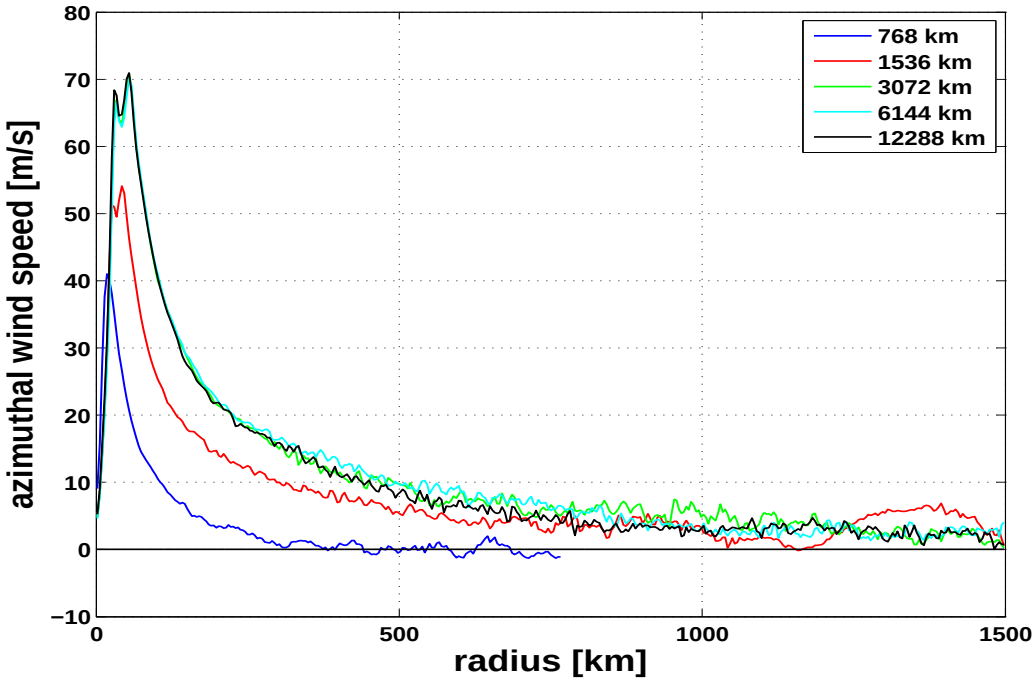

FIG. 2. Equilibrium radial gradient wind profiles as a function of domain width. Note the convergence beyond $L_{domain} \approx 3000\ km$.

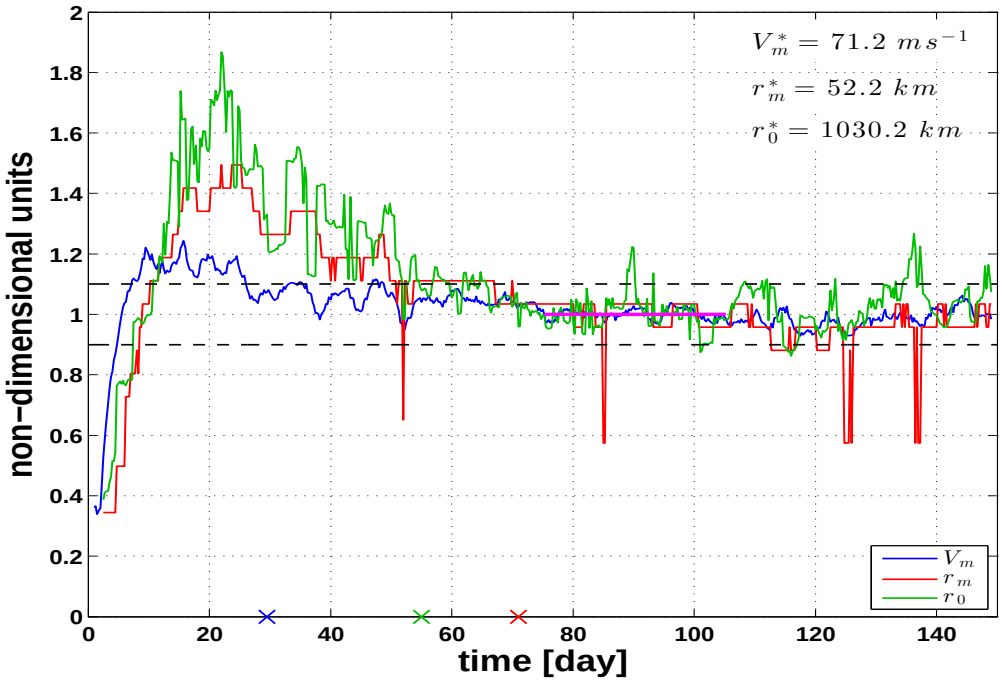

FIG. 3. For the Control simulation, time evolution of the 2-day running mean V_m, r_m, and r_0 normalized by their respective equilibrium values (upper-right corner). For this simulation, $V_p^* = 93\ ms^{-1}$ and $f = 5 * 10^{-5}\ s^{-1}$. Pink line denotes 30-day period used for equilibrium calculation. Markers along the x-axis denote respective time-scales to equilibration, defined as time where the 30-day running mean is within 10% of the equilibrium value (black dashed lines).

.

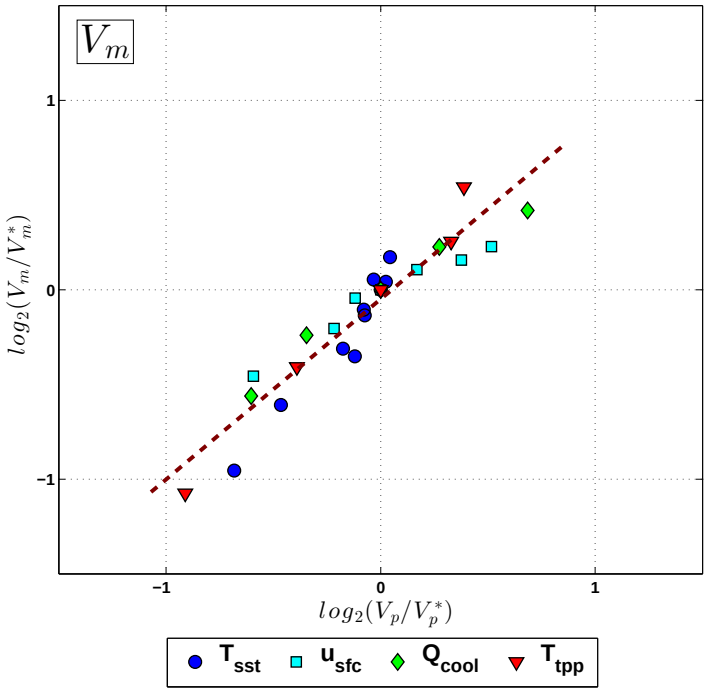

FIG. 4. Scaling of the equilibrium value of V_m (ordinate) with the potential intensity (abscissa). Both quantities are normalized by their respective control values denoted by an asterisk ($*$; $V_p^* = 93\ ms^{-1}$). Colored shape denotes the input parameter varied from among the four parameters on which the potential intensity depends (Eq. (7)). Scaling is shown in base-2 log-log space, such that a 1-unit increase (decrease) represents doubling (having). Thus, a straight line with unit slope indicates that a doubling of V_p is associated with a doubling of Y.

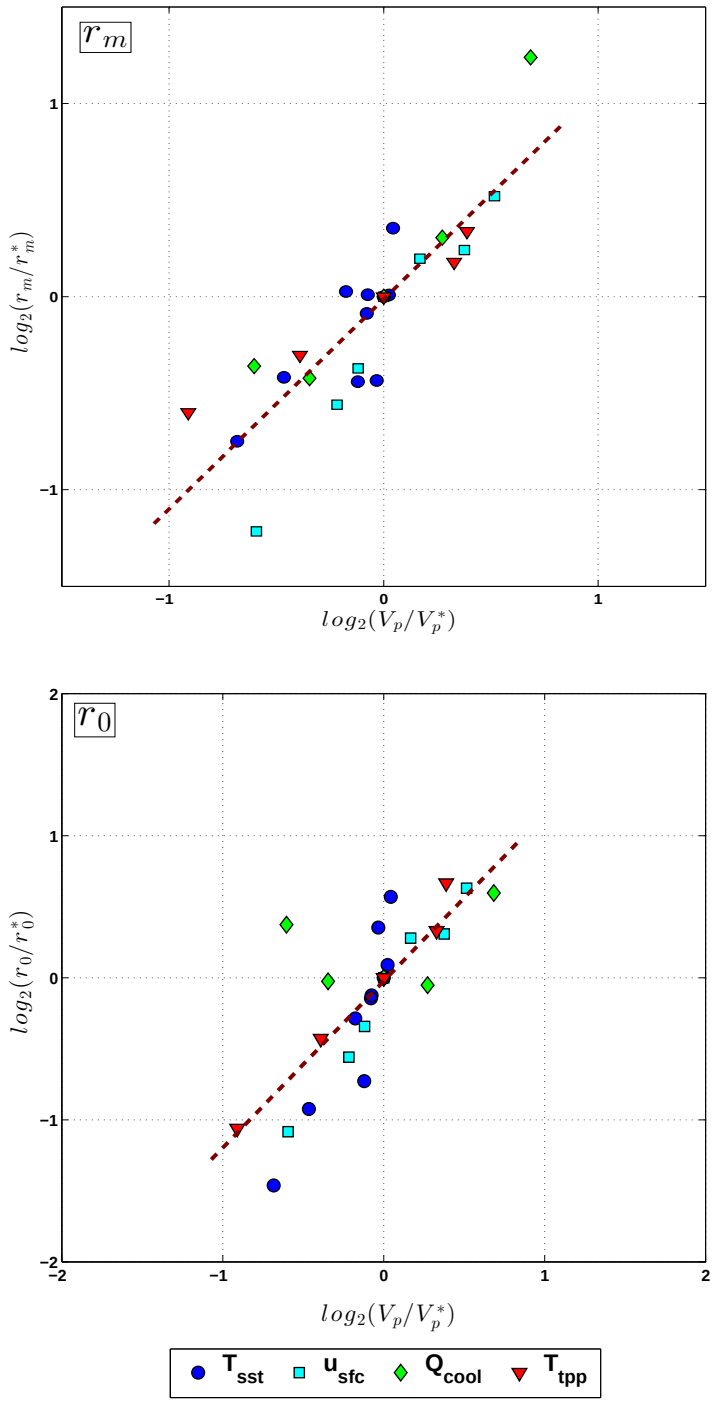

FIG. 5. As in Figure 4, but for r_m (top) and r_0 (bottom).

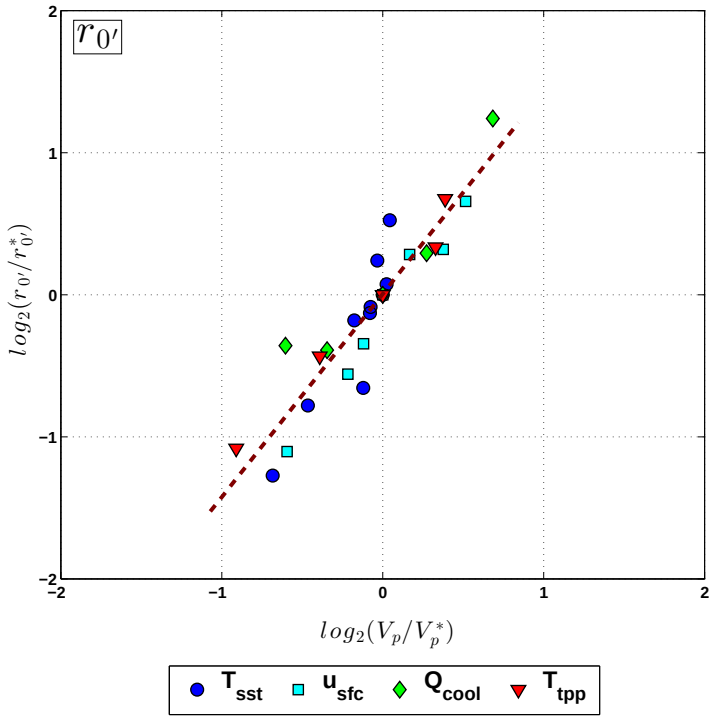

FIG. 6. As in Figure 5, but where $r_{0'}$ is r_0 calculated from (9) using the control value of w_{cool}.

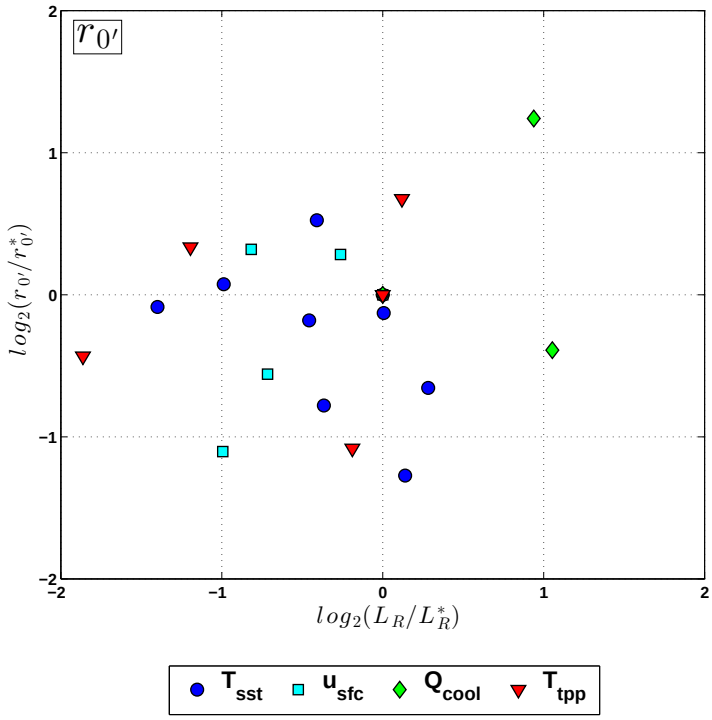

FIG. 7. As in Figure 6, but for the scaling with the Rossby deformation radius.

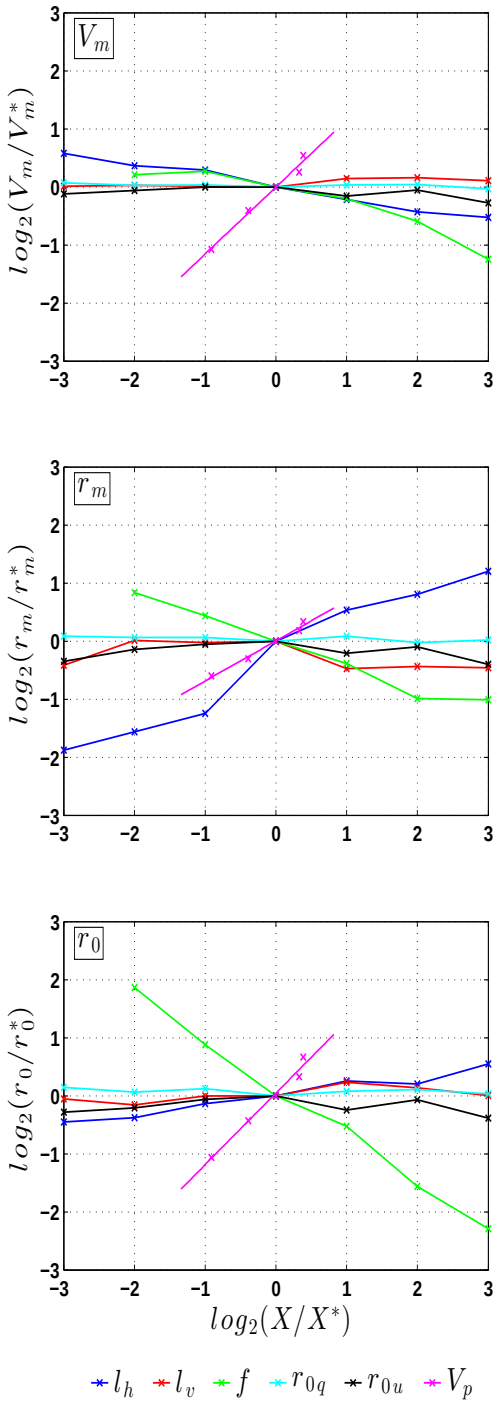

FIG. 8. Scaling of the equilibrium value of each structural variable Y (ordinate) with relevant dimensional parameters, X (absicssa). All quantities are normalized by their respective control values denoted by an asterisk ($*$). Plot layout as in Figure 4.

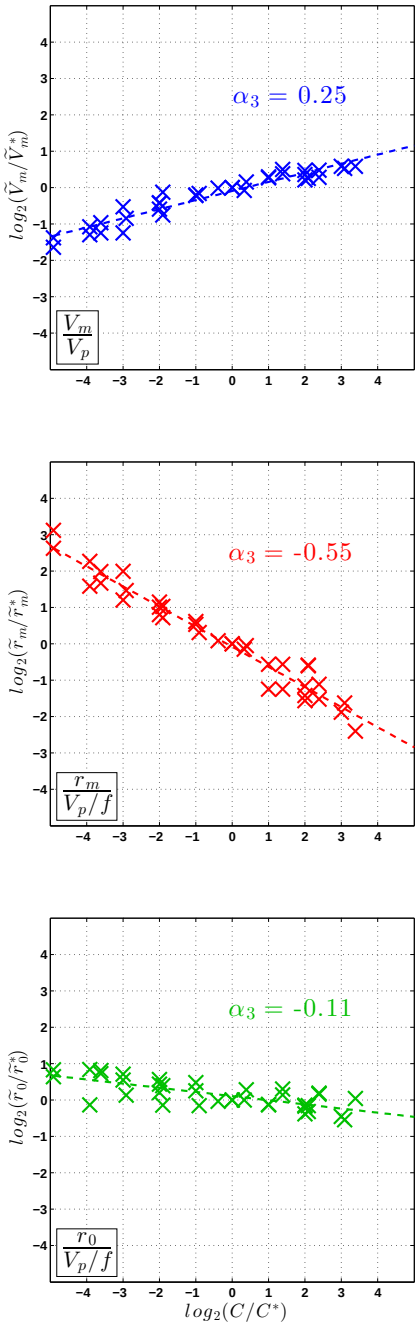

FIG. 9. Scaling of the equilibrium value of each structural variable non-dimensionalized by an appropriate dimensional scale (V_p for V_m; $\frac{V_p}{f}$ for r_m and r_0), Y, with the non-dimensional number $C = \frac{V_p}{f l_h}$ (see text for details). All quantities are normalized by their respective control values denoted by an asterisk ($*$; $C^* = 1240$). Plot layout as in Figure **??**. Linearly-regressed slopes, corresponding to the estimated scaling exponent in (12), and associated p-values shown in red.

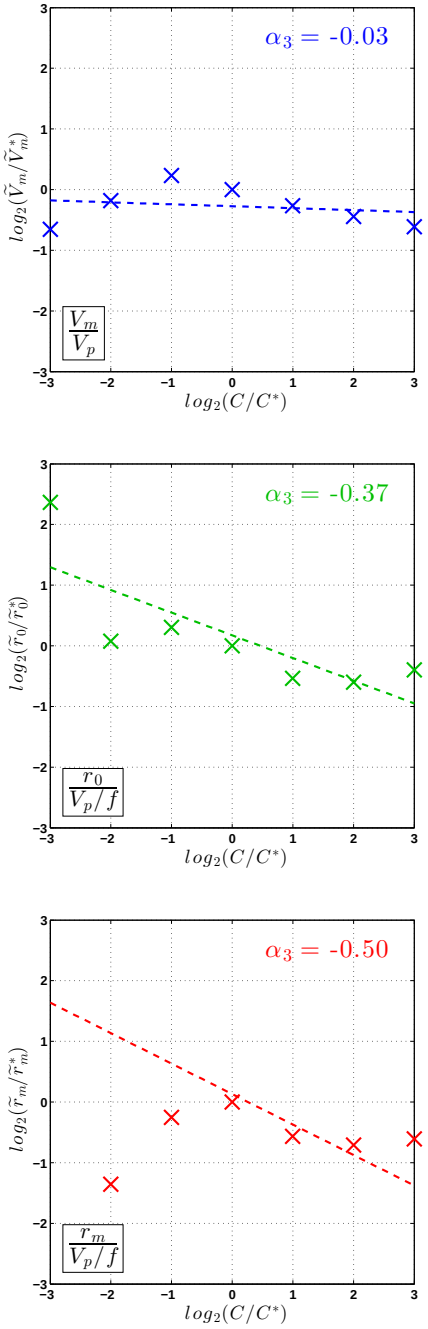

FIG. 10. As in figure 9, but for scaling with the non-dimensional ratio of exchange coefficients, $\frac{C_k}{C_d}$.

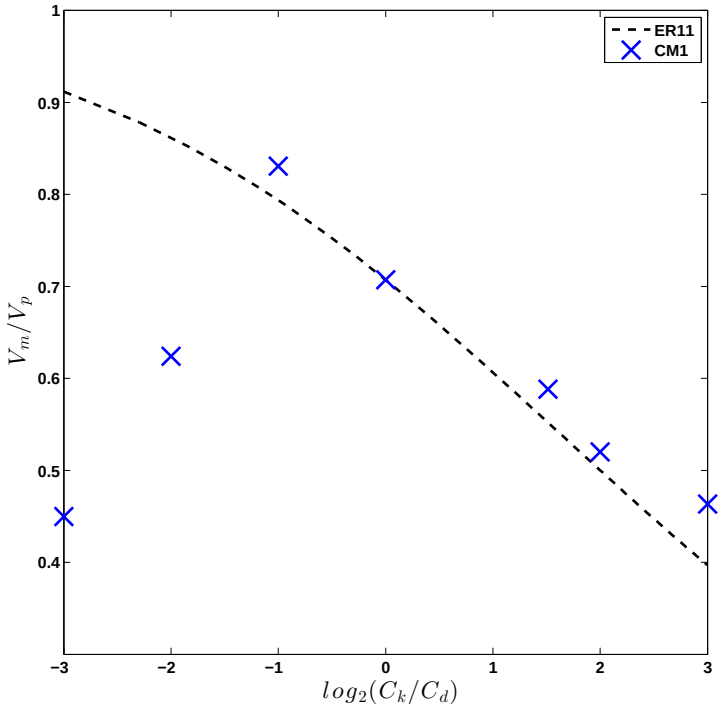

FIG. 11. Relationship between of $\frac{V_m}{V_p}$ and $\frac{C_k}{C_d}$ in simulations (markers) and the theoretical relation given by Eq. (41) of Emanuel and Rotunno (2011).

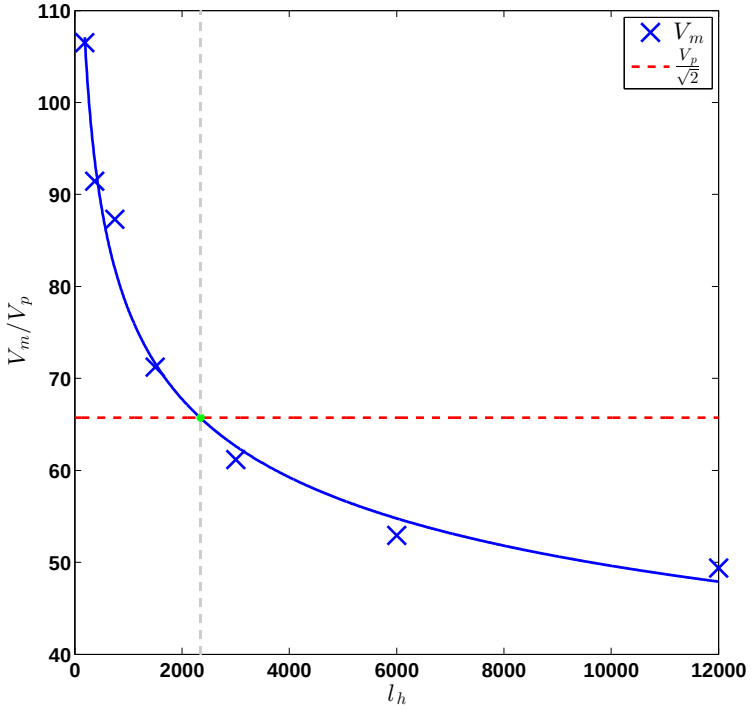

FIG. 12. Dependence of V_m on l_h. Matching a power-law fit of the data (solid blue line) to the theoretical relationship between V_m and V_p (dashed red line) given in Emanuel and Rotunno (2011) leads to a best-estimate value for l_h of 2350 m (green dot).